

# Evaluation of Static Capacity of Deep Foundations from Statnamic Testing

**REFERENCE:** Brown, Dan A., "Evaluation of Static Capacity of Deep Foundations from Statnamic Testing," *Geotechnical Testing Journal*, GTJODJ, Vol. 17, No. 4, December 1994, pp. 403-414.

**ABSTRACT:** A new method of load testing, called statnamic, is evaluated with respect to conventional methods of static load testing. Case histories are examined that provide a basis for comparison of static capacity as estimated from statnamic measurements with that of conventional load-deflection measurements. When evaluated using the simple procedure proposed by Middendorp, the statnamic method is shown to predict load-deflection response that is relatively close to that measured with conventional static load tests in most cases. Comparisons with conventional static load tests outlined in this paper suggest that excellent agreement can be obtained in sandy soils, but that the current evaluation procedure may tend to overpredict capacity by as much as 30% in stiff, overconsolidated clays.

**KEYWORDS:** piles, drilled shafts, load tests, instrumentation, statnamic method

## Nomenclature

The following symbols are used in this paper:

- $a$  acceleration
- $C$  viscous damping factor, a constant of proportionality between damping force and velocity
- $F_a$  the force due to inertia,  $= ma$ , mass times acceleration
- $F_{stn}$  the statnamic load, i.e., the measured force on the load cell
- $F_u$  the static soil resistance derived from the statnamic measurements
- $F_v$  the force due to damping,  $= Cv$
- $m$  mass
- $t$  time
- $t_4$  time at which maximum statnamic load ( $F_{stn}$ ) occurs
- $t_{umax}$  time at which maximum displacement occurs
- $v$  velocity

## Introduction

The high cost and large amount of time involved in setting up and conducting static load tests (particularly with high-capacity drilled shafts) has prompted a search for alternative methods of load testing that might be more efficient, quicker, and/or cost

effective. One such alternative that is beginning to be used commercially is the statnamic method, developed by Berminghammer Corp. of Canada and TNO Building & Construction Research of the Netherlands. This paper is intended to provide an independent review of the statnamic method, particularly with respect to the use of this method to provide a measure of static load capacity of deep foundations. The author has not been involved in the development of the statnamic device or testing method.

## Overview of the Test Procedure

The statnamic test is one in which the downward directed force on the pile top is mobilized by launching a reaction mass with fast-expanding, high-pressure gases in a cylinder, as shown in Fig. 1. By launching the reaction mass upward with an acceleration of 20  $g$ , for example, the downward force on the pile is thus on the order of 20 times the reaction weight. The duration of the load, the loading rate, and the total load applied can be controlled with the cylinder, piston, and fuel as well as with the amount of reaction mass. As of 1993, loads of up to 14.5 MN have been applied to a drilled shaft using the statnamic device. The load on the top of the pile is measured using a load cell, and the displacement is measured with a laser sensor. The velocity and acceleration of the pile is obtained by differentiation of the displacement/time measurement.

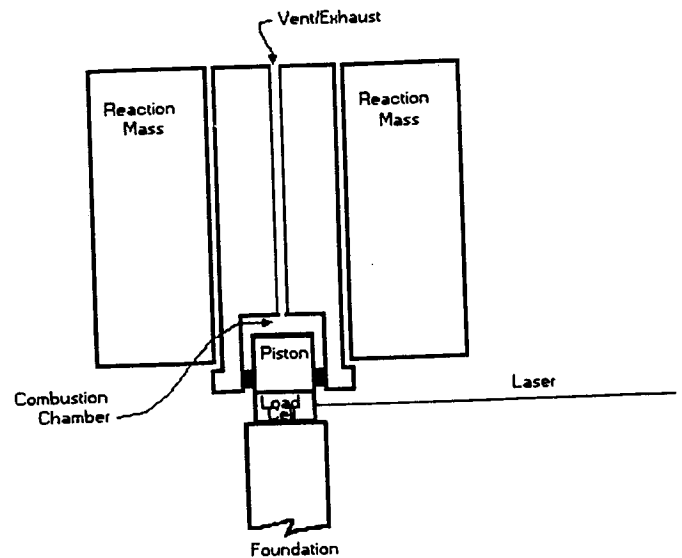


FIG. 1—Schematic of the statnamic loading device.

<sup>1</sup>Associate professor, Department of Civil Engineering, Auburn University, AL 36849.

The result of the statnamic launch is a relatively gentle push of the pile into the ground, which has a load duration much longer than that of an impact blow. An example of a load and displacement versus time measurement is provided in Fig. 2. The load rise time and duration is on the order of tens of milliseconds, an order of magnitude longer than a typical impact blow from a dynamic test. Given that the travel time of a stress wave down and back up a typical pile or shaft is on the order of a few (less than 10) milliseconds, it is clear that this type of loading will produce compression and downward movement of the entire pile or shaft at the same time. By contrast, an impact blow will result in the propagation of a compression stress wave through the pile such that a portion of the pile may be in compression and loading the soil, while another portion may be in tension and unloading. Tension stresses do not develop with the statnamic, and thus the load can normally be applied without concern regarding damage to the pile or shaft. By contrast with a conventional static load test, the rate of loading is still several orders of magnitude faster than is applied even with a quick-loading method. Dynamic effects such as inertia and damping are significant with the statnamic method and must be considered.

Although the actual field test procedure may appear to be more dramatic and exciting than conventional load testing, the procedure is relatively safe and quiet. The loading actually appears to produce less noise than a single pile hammer blow. The fuel used is not easily combustible, but rather is designed to produce a controlled burn; an individual fuel pellet can be lit with a match and burned on the ground without ill effects to bystanders. A surface wave propagates away from the test pile upon loading, which produces ground movement away from the test site. The relatively long wavelength (due to the long duration of the loading) and large amplitude produce a wave which can be felt a significant distance away from the test site; however, the long wavelength translates into quite low ground acceleration compared to blasting or pile driving, so that the effects on nearby structures are minimal. The most significant effect of the propagating surface wave is on the laser instrument; this instrument must be located at a sufficient distance from the test pile so that the surface wave arrival at the laser occurs after all relevant data are obtained (generally around 0.15 s).

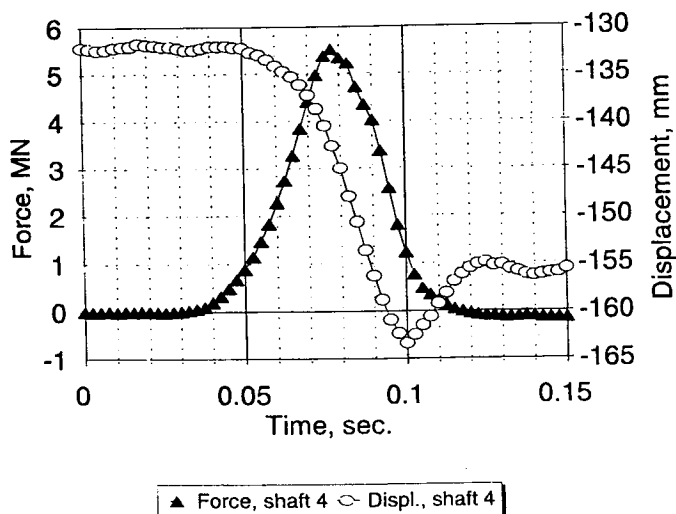


FIG. 2—Example of statnamic measurement.

## Interpretation of Statnamic Measurements and Computation of Static Capacity

The procedure used to evaluate statnamic measurements and to predict the static load versus deflection response is outlined by Middendorp et al. (1992) and briefly summarized below. This procedure has been utilized with the raw statnamic measurements of load and deflection in the case studies considered in this paper.

For the simplified modelling of the soil and pile behavior during the statnamic test, the pile or shaft is assumed to behave as a rigid body subjected to time-dependent forces and accelerations. Therefore, the time-dependent forces acting on the pile include:

1.  $F_{stn}$ , the statnamic load. This is a relatively straightforward measured quantity obtained during the test with the load cell.
2.  $F_a = ma$ , mass times acceleration, the mass of the pile times the acceleration of the pile. The mass of the pile is taken as a known quantity, although it is possible that a small amount of soil may adhere to the pile and could be included in this mass. The acceleration of the pile is obtained by twice differentiating the deflection measurements as a function of time. Some smoothing or averaging of the deflection-time data is typically used to obtain acceleration.
3.  $F_u$ , the soil resistance related to the static capacity of the soil. Although damping effects are treated separately, note that this is an undrained loading of short duration, so the pore pressure response of the soil and its effect on load transfer in side friction is a potential rate effect which would not be included as a part of damping.
4.  $F_v = Cv$ , damping factor times velocity, the soil resistance related to damping. The velocity of the pile is obtained by differentiating the deflection measurements as a function of time. As for the acceleration, some smoothing or averaging of the deflection-time data is typically used to obtain velocity. The damping factor,  $C$ , is taken as a constant of proportionality between force and velocity and therefore treats this as a viscous damping force.

Note that for dynamic analysis of pile driving it is common to attempt to separate end bearing and side friction in terms of both static resistance and damping; with this method, end bearing and side friction are lumped together.

For equilibrium

$$F_{stn}(t) = F_u(t) + F_v(t) + F_a(t) \quad (1)$$

or, in terms of static capacity,  $F_u$

$$F_u(t) = F_{stn}(t) - F_a(t) - F_v(t) \quad (2)$$

A plot of statnamic load versus deflection, which includes significant dynamic components, is presented in Fig. 3. On this figure, five areas are identified as follows:

1. Area 1 represents the assemblage of the statnamic device, including the reaction mass, atop the pile. The weight of these components results in a small initial static load and deflection.
2. Area 2 represents the initial elastic portion of the load-deflection response during the statnamic launch.
3. Area 3 represents the progression of the load-deflection response through the nonlinear range to a maximum statnamic load. Provided that this load is sufficient to overcome the ultimate soil resistance, the full static capacity of the pile would be reached during this phase.

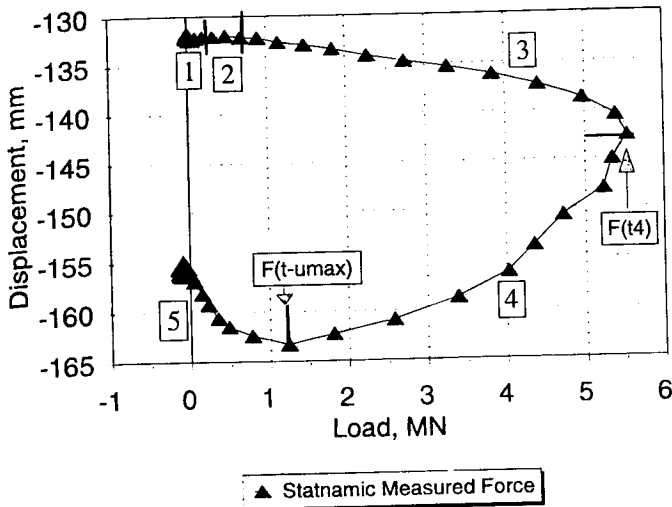


FIG. 3—Example of statnamic load-displacement measurement.

4. In Area 4, the statnamic load is decreasing; however, due to the inertia of the pile mass, downward displacement continues with the full static capacity of the pile mobilized through this phase. At the end of Area 4 (time =  $t_{umax}$ ), the displacement reaches a maximum and the pile velocity is zero.
5. Area 5 represents the unloading and rebounding of the pile or shaft. If the full static capacity has been mobilized, permanent displacement would result.

The points at the end of Areas 3 and 4 are critical for evaluation of the statnamic test. At the end of Area 4, the velocity will be zero, and thus the damping force,  $F_v$ , would be zero. Therefore, at time  $t_{umax}$ , Eq 2 simplifies to

$$F_u(t_{umax}) = F_{sin}(t_{umax}) - F_a(t_{umax}) \quad (3)$$

In order to calculate  $F_u$  as a function of time (and therefore as a function of displacement),  $F_v(t)$  must be known. Damping can be computed based on the response in Area 2 using the stiffness determined in Area 1 during assembly of the reaction mass. However, of more interest is the damping in Area 4 near the point of maximum soil resistance. Assuming that: (a) the full static resistance is mobilized at the end of Area 3, and (b) the damping can be characterized using a viscous damping coefficient,  $C_4$ , then, within Area 4,  $F_u$  would be a constant and Eq 1 can be written as

$$F_{sin}(t) = F_u(t_{umax}) + C_4 v(t) + ma(t) \quad (4)$$

where

- $F_u(t_{umax}) = F_u(t)$  within Area 4, which is assumed constant in this region for purposes of computing damping,
- $C_4 v(t) =$  damping coefficient  $C_4$  times the measured velocity =  $F_v(t)$  within Area 4,
- $ma(t) =$  mass of the pile or shaft times the measured acceleration (actually acceleration derived from the measured velocity) =  $F_a(t)$  within Area 4.

Using the values of time-dependent quantities at the point of maximum statnamic load (time =  $t_4$ ) and rearranging Eq 4

$$C_4 = \frac{[F_{sin}(t_4) - F_u(t_{umax}) - ma(t_4)]}{v(t_4)} \quad (5)$$

where

- $F_{sin}(t_4) =$  the maximum statnamic load (which occurs at time  $t_4$ ),
- $F_u(t_{umax}) =$  the static soil resistance computed from Eq 3 as the statnamic load at maximum displacement adjusted for acceleration at maximum displacement,
- $ma(t_4) =$  mass  $\times$  acceleration at time ( $t_4$ ), and
- $v(t_4) =$  velocity at time ( $t_4$ ).

With this value for  $C_4$ , the static soil resistance  $F_u(t)$  for a range of time values,  $t$ , can be computed using Eq 4, and, with displacement  $u(t)$ , a relationship between static soil resistance and displacement is established.

### Case Studies of Statnamic Load Tests

In order to critically evaluate the statnamic load test method, it is important to evaluate test sites where measurements are available using both the statnamic and conventional load test methods where load tests to failure are available. The author has evaluated data for eight such load tests at each of six test sites. The test sites provide a fairly wide range of soil conditions. All of the sites are in the continental United States and Canada, and all but one test were loaded at or near to failure of the pile or shaft. All of the data are from tests of drilled shaft or auger cast piles; although the method is readily adapted to driven piling, the test data on driven piling that were available to the author either did not result in plunging failure of the pile or were incomplete in some aspect. The statnamic load test data were obtained by the author directly from Patrick Bermingham of Bermingham Corp.; these data were in engineering units as provided from the field data acquisition computer, but were otherwise raw load and deflection measurements. All analyses of the data to produce the computed static load-deflection and other plots presented in this paper have been performed by the author following the procedure outlined above.

#### I-40 at Rio Puerco, Gallup, N.M.

A 0.76-m-diameter by 13.8-m-deep drilled shaft installed in a dry clayey soil was subjected to a static load test to failure followed by statnamic testing. Soil conditions consist of very stiff silty clays and clayey silts with standard penetration test blow counts (b), typically in the range of 17 to 32 b/ft (b/300 mm) and moisture contents typically in the range of 8 to 19%. During the static test of 1 April 1993, the shaft appeared to plunge at a load of 3.65 MN to a maximum displacement of just over 13 mm. Note that this plunging failure at a relatively modest displacement is characteristic of load tests in clays. Statnamic testing was performed on the same shaft on 5 April 1993. Load versus displacement curves for both tests are shown in Fig. 4 with the predicted static response computed using the Middendorp procedure with the statnamic test data. Note that the recorded permanent set at the end of the static test is used as the start of the statnamic test.

Shown in Figs. 5 and 6 are the measured statnamic loads and displacements with the computed velocity and acceleration as a function of time. Note that the accelerations are quite low until the maximum downward velocity is reached (negative velocity); the greatest acceleration felt by the shaft is during deceleration as the shaft comes to a halt. The velocity crosses the zero axis a short time after the peak statnamic force occurs.

Using the statnamic load at the point of zero velocity and

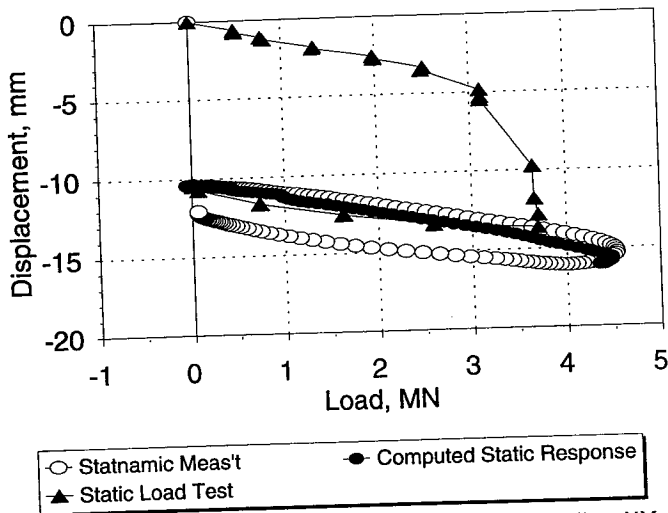


FIG. 4—Load versus displacement, I-40 at Rio Puerco, Gallup, NM.

adjusting for the mass times acceleration of the shaft, the statnamic test provides an estimated static resistance of around 4.5 MN. The adjustment for damping allows computation of the estimated load-displacement plot provided in Fig. 4. These data suggest that the procedure used with the statnamic data either overestimated the static resistance by about 25% or that the static component of the resistance during the statnamic loading event was somewhat higher than during the previous static load test. Of course, some strain hardening might occur with a second loading of a drilled shaft.

*I-40 at Rio Grande, Albuquerque, N.M.*

A 0.76-m-diameter by 18.3-m-deep drilled shaft installed in a sandy soil was subjected to static load testing to failure followed by statnamic testing. The soil conditions at this site consist of a highly variable deposit of very loose to dense poorly graded sands, silty sands and gravel with thin layers of silt, with groundwater at around 3 to 5 m in depth. The test shaft was installed using a bentonite slurry. The static load testing in this case included a compression test to failure followed by a pullout test to failure,

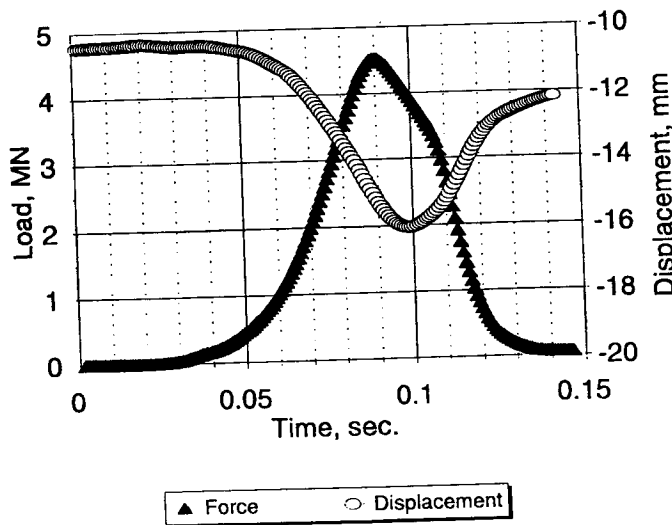


FIG. 5—Load and displacement versus time, I-40 at Rio Puerco, Gallup, NM.

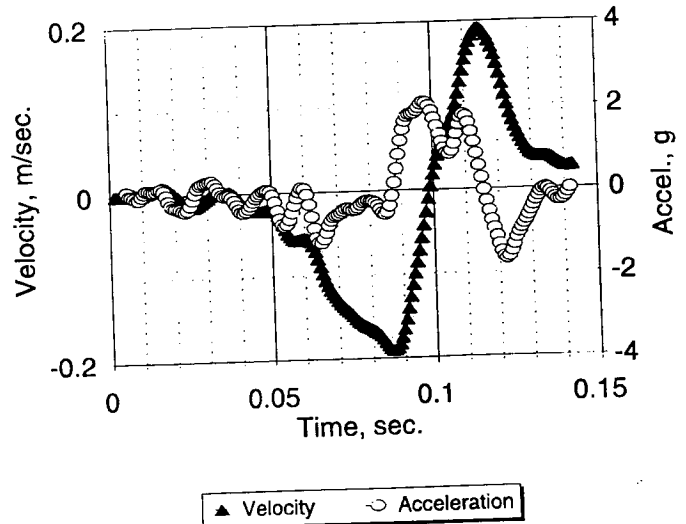


FIG. 6—Velocity and acceleration versus time, I-40 at Rio Puerco, Gallup, NM.

with statnamic testing performed after the pullout test. During the initial compression test, the shaft did not appear to “plunge,” but was loaded to a displacement in excess of 50 mm at a load of 8.4 MN. The shaft was subsequently pulled to an uplift failure load of around 1.7 MN with a final permanent set of a bit less than 13 mm below the initial position as indicated by the load-displacement curve in Fig. 7. One would thus expect that end bearing might be contributing to a large portion of the capacity in compression. Statnamic testing was performed on the same shaft 42 days later on 16 Sept. 1992 and again on 20 Sept. 1992. Load versus displacement curves for all tests are shown in Fig. 7, along with the predicted static response computed using the Middendorp procedure with the statnamic test data. Note that the recorded permanent set at the end of the static testing is used as the start of the statnamic test.

Shown in Figs. 8 through 11 are the measured statnamic loads and displacements along with the computed velocity and acceleration as a function of time for both statnamic loadings of this shaft. Note that the large displacement rebound at and beyond 0.14 s for Loading No. 2 is not realistic as it would require a huge sudden acceleration upward; these data points are likely due to errors in

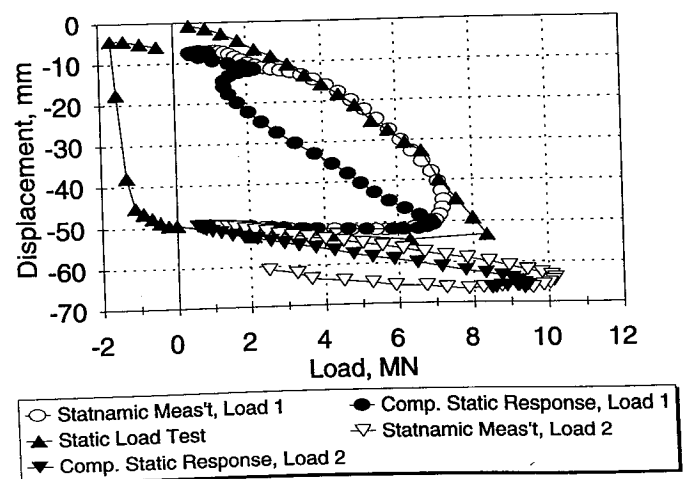


FIG. 7—Load versus displacement, I-40 at Rio Grande, Albuquerque, NM.

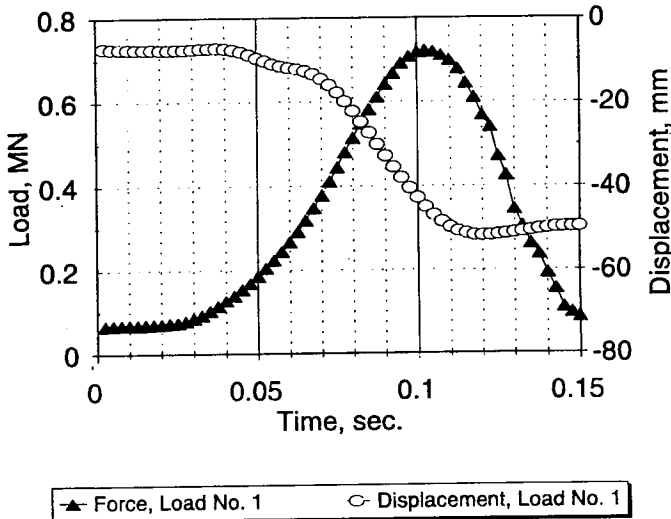


FIG. 8—Load and displacement versus time, Load 1, I-40 at Rio Grande, Albuquerque, NM.

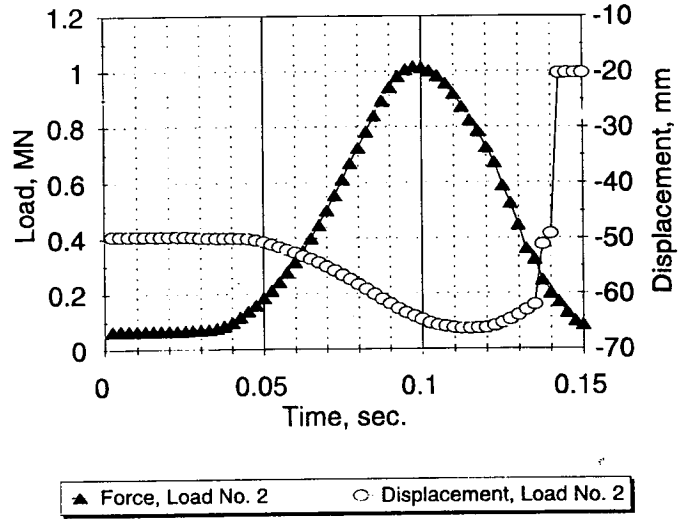


FIG. 10—Load and displacement versus time, Load 2, I-40 at Rio Grande, Albuquerque, NM.

the laser displacement measurement. At some time after the initial statnamic launch, the surface waves propagating away from the test shaft will affect the laser; thus, it is important that the displacement instrument be sufficiently distant from the test shaft to capture the relevant portion of the signal before the arrival of dynamic ground motions.

At this site the statnamic load response is significantly affected by the prior static load test sequence, particularly the pullout test. Because of the pullout test, a downward displacement to around 50 mm or so is required to “remobilize” the end bearing component of the static resistance. The first statnamic loading appears to have used all of the statnamic load energy reloading the shaft to approximately the position of the initial compression loading. The “hitch” in the computed static resistance at a displacement of -13 mm may well correspond to full mobilization and failure of the side friction of a shaft that has a void beneath the toe. Note that this point corresponds to a reversal in velocity for Statnamic Load 1 (Fig. 9) at 0.04 to 0.05 s. While simple data errors cannot be completely ruled out, this reversal is unusual in the author’s experience; this anomalous fluctuation in velocity and acceleration

appears to coincide with the mobilization of side friction mentioned above.

After the first statnamic loading recovered the base resistance, the second statnamic loading appears to represent a reloading cycle as might reasonably be expected for a subsequent static reloading cycle. A computed static resistance of approximately 9.8 MN is mobilized at a displacement of approximately 64 mm from the initial position. Although this value exceeds the maximum load from the static load test, the load-displacement response did not have the characteristic of a plunging failure, and a subsequent increasing load with increasing displacement on a reload cycle appears entirely plausible for this test site.

*Auger Cast Piles, Barrie, Ontario*

This was the site of a multistory apartment building founded on a 0.46-m-diameter auger cast piling. The test piles extend to an embedded length of 11.6 m through a weak surficial layer of heterogeneous fill and organic soil some 5 to 8 m thick to bear

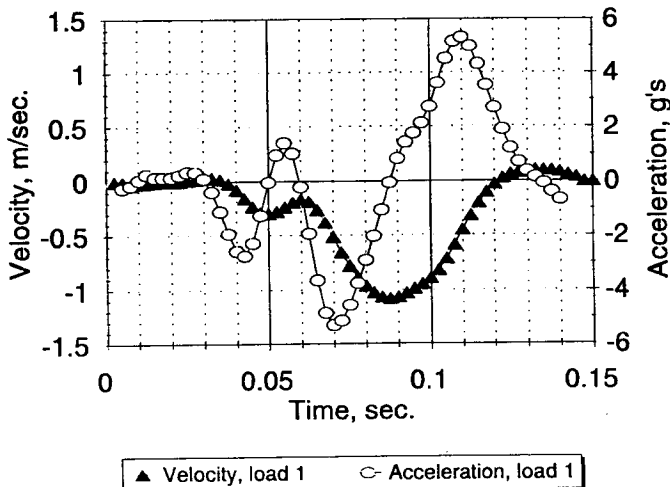


FIG. 9—Velocity and acceleration versus time, Load 1, I-40 at Rio Grande, Albuquerque, NM.

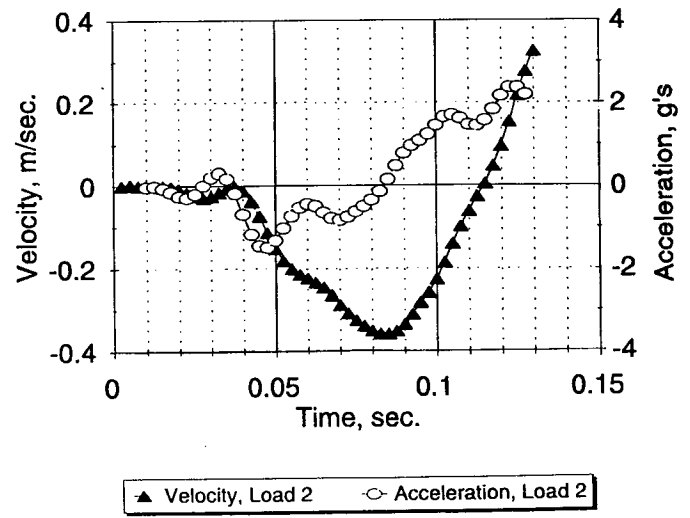


FIG. 11—Velocity and acceleration versus time, Load 2, I-40 at Rio Grande, Albuquerque, NM.

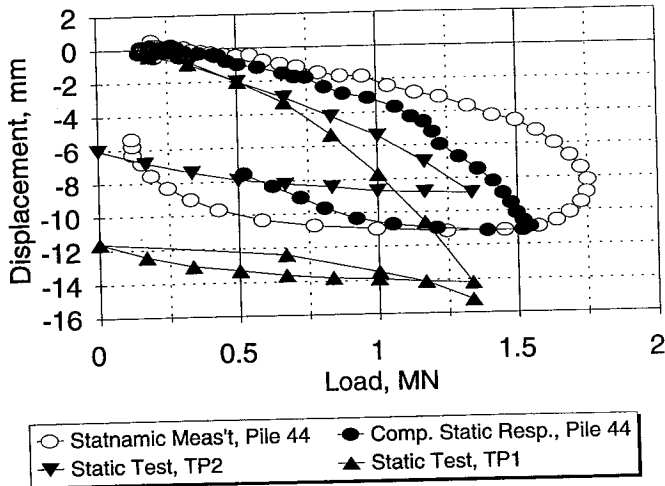


FIG. 12—Load versus displacement, Auger Cast Piles, Barrie, Ontario.

in a medium dense sandy silt or silty fine sand. Groundwater was at a level approximately 3 m below the surface of the fill. Conventional static tests were performed on two auger cast piles with statnamic testing performed on another nearby pile. Actually, two statnamic tests were performed on different piles, but the results appeared to be so similar that only the test data for Pile No. 44 is presented here.

Load versus displacement curves for the two static test piles and for the statnamic test pile are presented in Fig. 12, along with the computed static load-displacement response from the statnamic measurement. Neither of the static tests exhibited a plunging-type failure. The computed static response from the statnamic measurement appears similar in shape and slightly stiffer. Because these represent three different piles, some variation between piles can be expected as indicated by the difference in the two static load tests; it is possible that the statnamic test pile actually was slightly stiffer. Nevertheless, the data suggest that the statnamic test overpredicts stiffness and capacity at this site, although only by a small amount. Load, displacement, velocity, and acceleration time histories are presented in Figs. 13 and 14. These time history curves appear normal compared to other observed time histories.

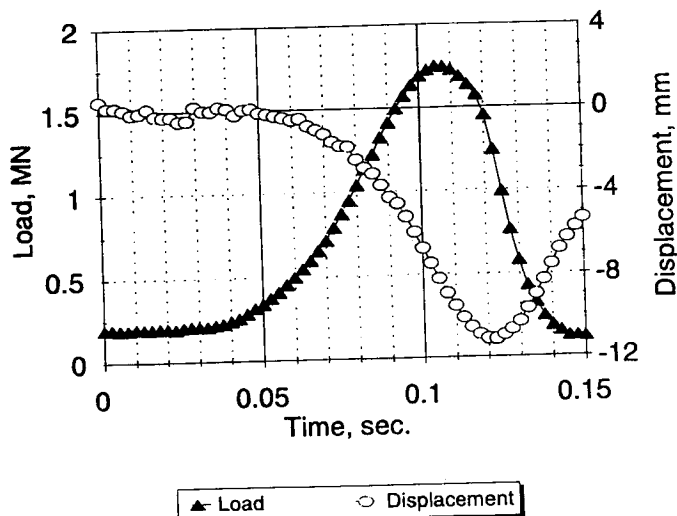


FIG. 13—Load and displacement versus time, Auger Cast Piles, Barrie, Ontario.

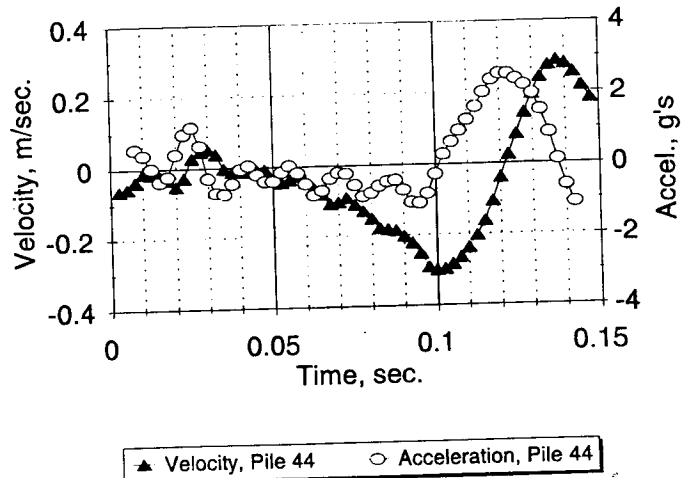


FIG. 14—Velocity and acceleration versus time, Auger Cast Piles, Barrie, Ontario.

### 36-in. Drilled Shafts, Cupertino, California

Two 0.9-m-diameter by 9.1-m-deep drilled shafts were tested in a dry sandy soil at a site in the CalTrans maintenance yard in Cupertino, California. The drilled shafts at this site were constructed as a part of an FHWA research project into integrity testing and dynamic measurement of capacity. The soil conditions at this site consist of alternating layers of very dense clayey and sandy gravels to a depth of approximately 10 m underlain by dense silty sands and sands. Groundwater was well in excess of 10 m deep. Both shafts were constructed in the dry using conventional earth auger equipment. One of the shafts (Shaft 4) was constructed to have a soft bottom condition, while Shaft 2 was constructed with good construction practice. Conventional static and subsequent statnamic tests were performed on both. Shaft 2 (the good shaft) supported a load of over 7.5 MN during static loading, and the capacity of this shaft substantially exceeded the capacity of the 5.3 MN statnamic device used for this project. The shaft with the soft bottom condition was loaded to a significant displacement by the static and subsequent statnamic loadings; load-displacement measurements along with computed static response from the statnamic loading are presented in Fig. 15. Load, displacement, veloc-

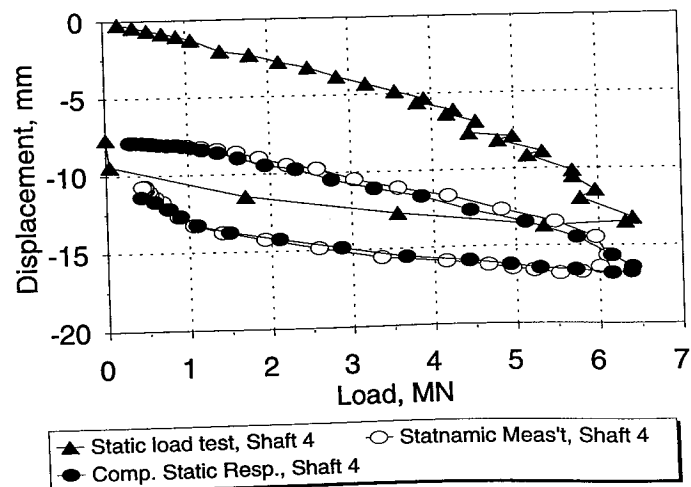


FIG. 15—Load versus displacement, Cupertino, CA.

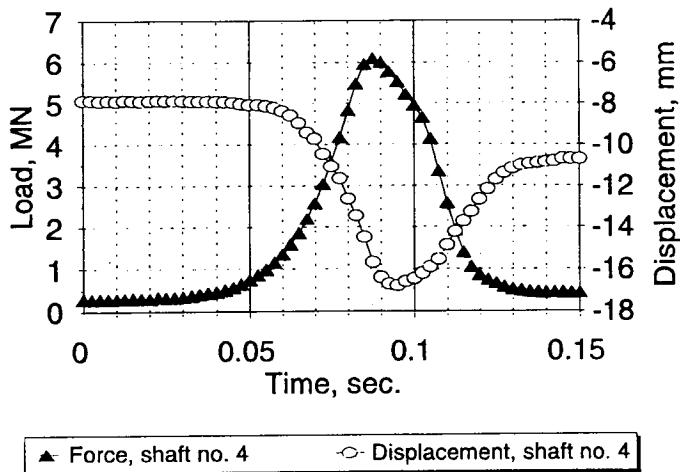


FIG. 16—Load and displacement versus time, Cupertino, CA.

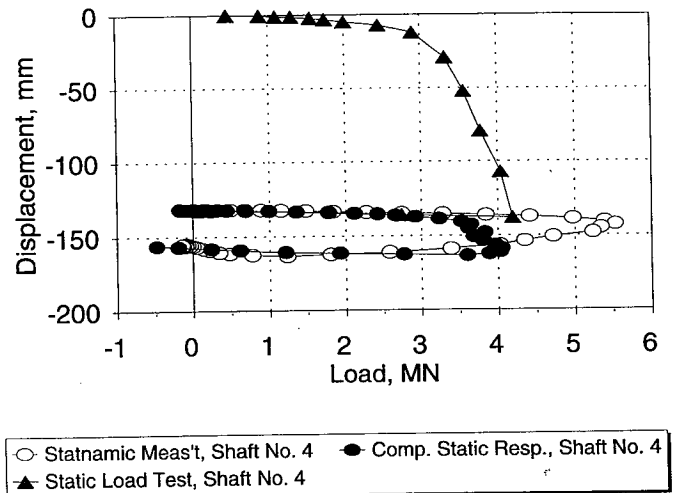


FIG. 18—Load versus displacement, Shaft 4, College Station, TX.

ity, and acceleration time history plots are provided in Figs. 16 and 17.

Although the load-displacement plot did not exhibit a plunging failure for either loading, the load displacement curve for the static loading becomes increasingly nonlinear beyond 5.3 MN. The statnomic loading and computed static resistance from this test suggests a reasonable reload load-displacement plot for this test. The fact that the shaft was not loaded to failure is reflected in the rebound exhibited in both Fig. 15 and on the displacement time-history in Fig. 16.

*FHWA Research, Texas A&M, College Station, Texas*

Three drilled shafts (Shafts 2, 4, and 7) were load tested by both static and statnomic methods as a part of a research program into integrity testing and dynamic methods for predicting capacity. Details of the shaft construction, loadings, and soil conditions are presented by Ballouz et al. (1991). Each of these shafts were statically loaded to very large displacements to ensure that both end bearing and side friction were fully mobilized. Statnomic testing was performed in each case as a reloading after the initial static load testing. The statnomic testing was performed "blind," i.e., the people performing the statnomic tests were unaware of the results of the previous static load tests. Instrumentation was included to measure the load transfer along the shafts and in end

bearing during the static tests; however, the instrumentation was not monitored during statnomic loading. Each of the shafts represents a quite different set of soil conditions, as described below.

*Shaft No. 4, Wet Sand Site*—Shaft No. 4 was a straightforward drilled shaft installation using slurry at a site consisting of sand with a relatively shallow groundwater. The shaft was 0.9 m in diameter and embedded to a depth of 10.4 m. Soil conditions consist of medium dense fine sands and silty sands to a depth of approximately 13.4 m, underlain by stiff clay. Standard penetration test soundings in the sands typically ranged from 8 to 25 b/ft (b/300 mm). Groundwater was at a depth of around 7.6 m below grade. The overall load-displacement plot for the static and statnomic tests are shown in Fig. 18; because the shaft was loaded to such a large displacement, the load-displacement plot for the statnomic data is also shown in Fig. 19 at an enlarged scale. Load, displacement, velocity, and acceleration time histories are presented in Figs. 20 and 21.

Shaft No. 4 clearly exhibits a plunging-type failure during both the static and statnomic tests; Figs. 19 and 20 reveal a maximum displacement during statnomic loading of over 25 mm. Maximum static resistance indicated by the statnomic data is around 4 MN, which approaches the maximum measured load during the static

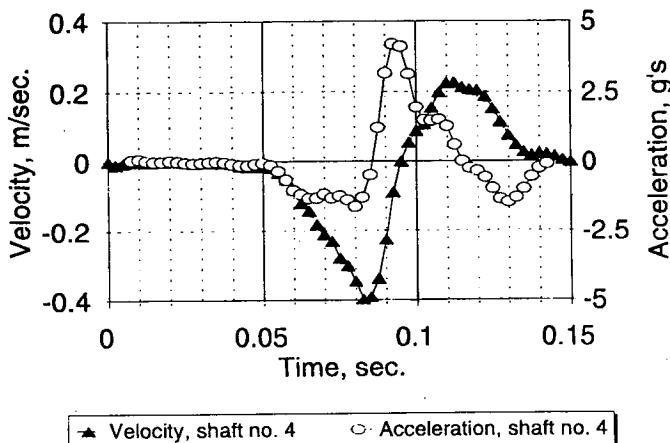


FIG. 17—Velocity and acceleration versus time, Cupertino, CA.

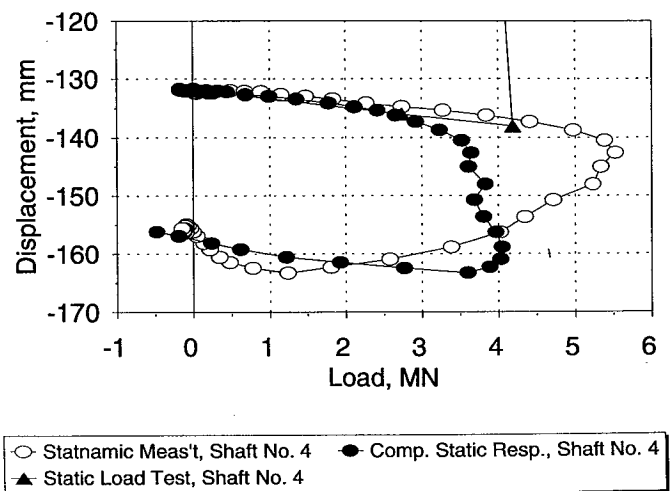


FIG. 19—Load versus displacement, Shaft 4, College Station, TX.

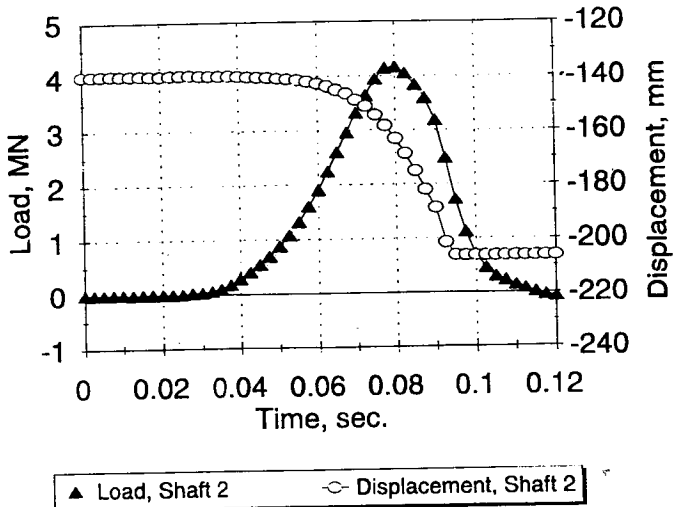
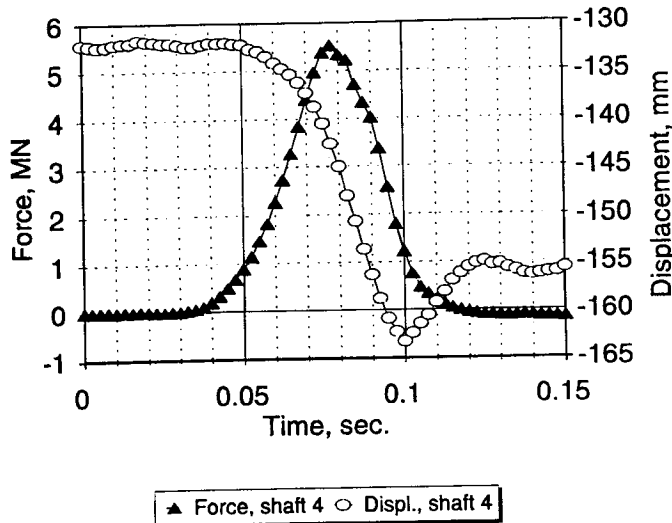


FIG. 20—Load and displacement versus time, Shaft 4, College Station, TX.

FIG. 22—Load and displacement versus time, Shaft 2, College Station, TX.

load test and appears to correspond reasonably well to the previous static loading given the relatively large displacement which occurred. Strain gage measurements during the static load testing indicate that the capacity of Shaft No. 4 is about 15% in end bearing.

The relatively large displacement observed during this statnamic loading illustrates the importance of obtaining good acceleration data for the test. The point of zero velocity is observed at a time of approximately 0.1 s. At that time, the statnamic load,  $F_{stn}$ , has dropped to 140 tons (1.3 MN), but the computed static resistance,  $F_s$ , is 3.6 MN. The substantial difference of 2.3 MN is due to the mass of the shaft times the acceleration (about 11.5 g). This portion of computed resistance is probably the greatest source of uncertainty and potential error with a relatively massive drilled shaft foundation. Although the acceleration response illustrated in Fig. 21 appears quite reasonable, errors in displacement measurements are amplified when twice differentiating to obtain acceleration. The smoothing used with the displacement data reduces the sensitivity to measurement errors, but introduces an additional variable into the static resistance computation.

In summary, the statnamic measurement for Shaft No. 4 at

the College Station, Texas wet sand site appears to be a good measurement, and the computed static soil resistance from the statnamic measurements correspond closely to the static load test measurements performed previously.

*Shaft No. 2, Mudcake Defects at Wet Sand Site*—Shaft No. 2 was constructed with an intentional defect in that the shaft was formed in an excavation which included a soft base and a thick mudcake layer separating the shaft and native sandy soil. The capacity of this shaft was thus greatly diminished relative to that of Shaft No. 4, which was otherwise similar (0.92 m in diameter by 10.4 m deep). Statnamic testers were unaware of the shaft defects and loaded the device with a load of fuel appropriate to a higher capacity shaft. Because of the relatively low capacity of Shaft No. 2 and the large applied statnamic force, the shaft was plunged to a large displacement during the test, as indicated on the plot of load and displacement versus time of Fig. 22. Note that the initial displacement is shown at -140 mm to reflect the previous static load test displacement. During the statnamic test, the relative deflection of the shaft exceeded the travel of the measuring system, so the values of displacement beyond 0.09 s are invalid. It is also the case, as shown in Fig. 23, that the point

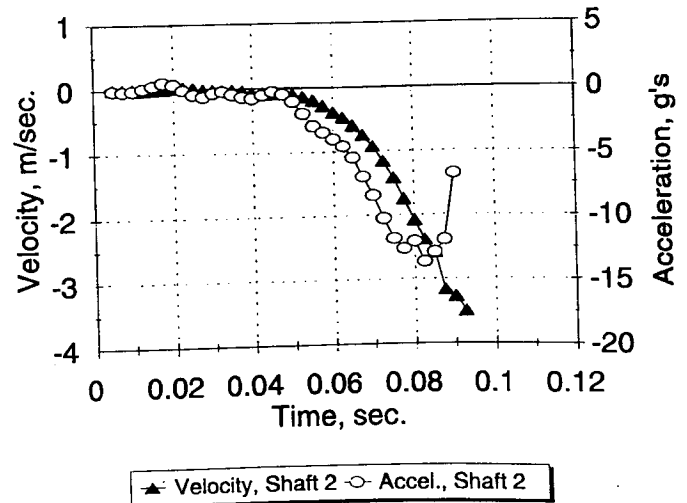
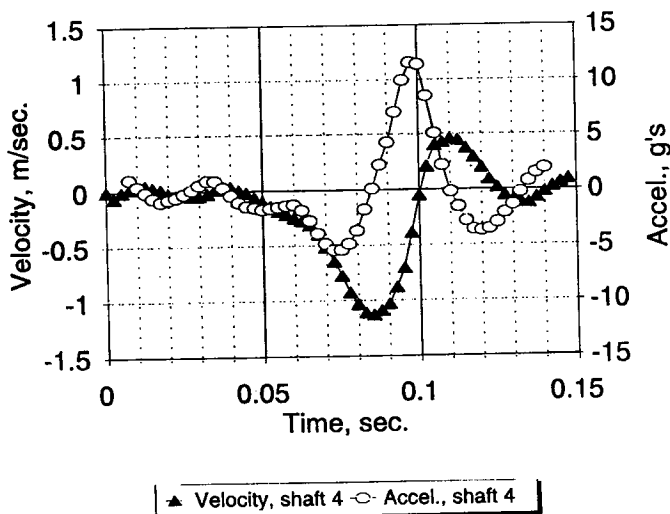


FIG. 21—Velocity and acceleration versus time, Shaft 4, College Station, TX.

FIG. 23—Velocity and acceleration versus time, Shaft 2, College Station, TX.

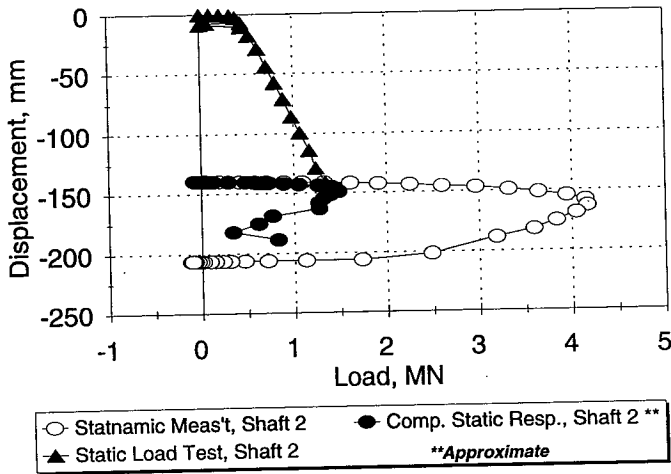


FIG. 24—Load versus displacement, Shaft 2, College Station, TX.

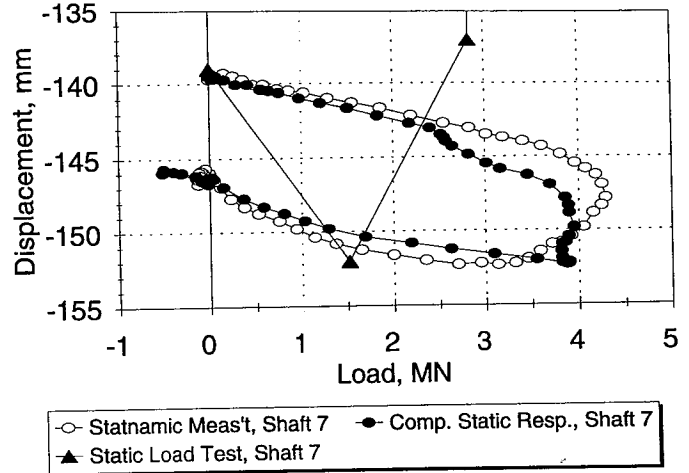


FIG. 26—Load versus displacement, Shaft 7, College Station, TX.

of zero velocity is not known and that the acceleration at the zero velocity point is not known.

Presented in Fig. 24 is a plot of the statnamic load versus displacement measurements along with the previous static load test and a computed static soil resistance from the statnamic data using an estimated dynamic soil resistance constant. Although interpretation of statnamic test data was not refined at the time of this test (1990), it is evident from the evaluation of the data using the current procedure that this test should have been repeated using a smaller fuel load and/or reaction mass. The approximate static resistance is computed using an estimate of  $C_4$  which appears to be within a reasonable range based on data from other tests; even using a relatively wide range of  $C_4$  values, the maximum static resistance is computed to vary by only about 30% about the maximum value shown. Additionally, it is evident from the measurements that the end of Area 4 has not been achieved at a statnamic load which has dropped to 1.8 MN; this observation constrains the range of possible static soil resistance to levels not exceeding those indicated. The estimated static response from the statnamic test appears to reflect a reloading condition for a shaft which exhibited "hardening" after loading to a permanent displacement of about 140 mm.

In summary, the statnamic test data for Shaft 2 are incomplete (likely due to an incomplete understanding of the test measure-

ments at the time the test was performed), but an approximate analysis using the Middendorp procedure suggests that reasonably good agreement exists between static soil resistance from the static load test and the interpretation of the statnamic data. This shaft is likely to represent an extreme situation and probably more closely resembles loading in a soft clay material than in the native sandy soil.

**Shaft No. 7, Stiff Clay Site**—Shaft No. 7 was drilled in the dry at a nearby site that consists of very stiff clay underlain by hard clay to depths of over 13 m. Undrained shear strengths as determined by conventional unconsolidated, undrained triaxial tests were in the range of 70 to 140 kPa. The shaft was constructed with no intentional defects to 0.92 m in diameter by 9.5-m depth. The statnamic load test was performed about four days after the static test. The overall load-displacement plot for the static and statnamic tests is shown in Fig. 25; because the shaft was loaded to such a large displacement, the load-displacement plot for the statnamic data is also shown in Fig. 26 at an enlarged scale. Load, displacement, velocity, and acceleration time histories are presented in Figs. 27 and 28.

Shaft No. 7 clearly exhibits a plunging-type failure during both the static and statnamic tests, although the maximum displacement

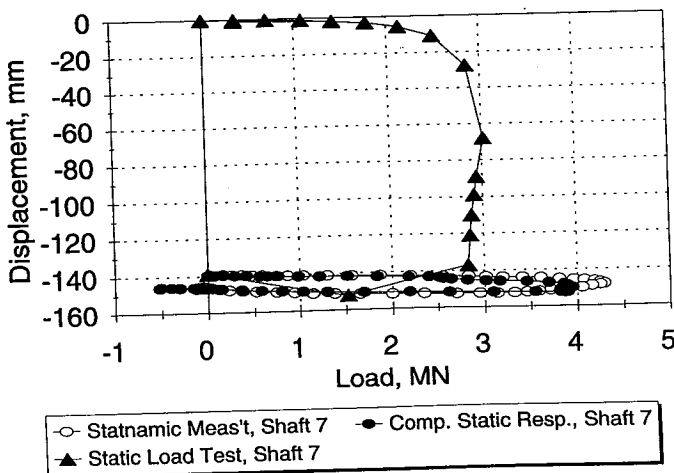


FIG. 25—Load versus displacement, Shaft 7, College Station, TX.

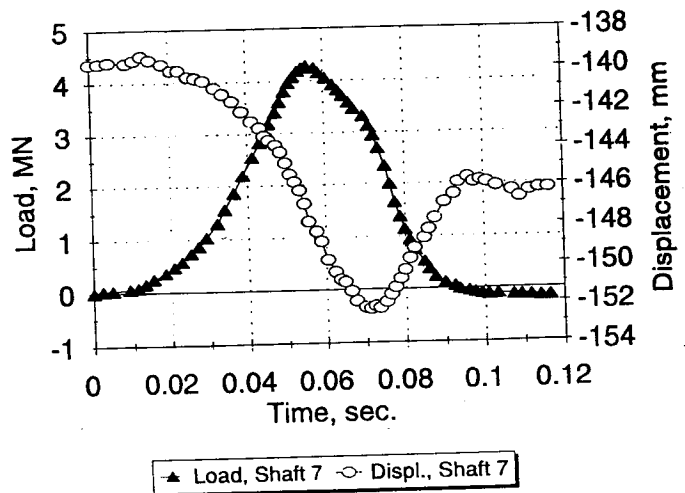


FIG. 27—Load and displacement versus time, Shaft 7, College Station, TX.

during statnamic loading was only about 13 mm. Maximum static resistance indicated by the statnamic data is around 3.9 MN. As was the case for the other statnamic test on a drilled shaft in stiff clay (Rio Puerco, New Mexico), the computed static soil resistance during the statnamic loading exceeds the maximum measured load during the static load test by about 30%. Time history measurements appear to suggest that good measurements were obtained and that the shaft responded typically as compared to other statnamic loadings of similar shafts. Strain gage measurements obtained during the static load test indicate that the shaft capacity was about one third end bearing.

In summary, the interpreted static soil resistance from the statnamic measurements for Shaft No. 7 exceeds the measured static soil resistance by a significant amount. This result is similar to the one other test to failure in a stiff clay and may suggest that either there is some component of static resistance related to the high rate of loading or that the soil damping is not adequately accounted for in these soils.

*I-49II-20 Interchange, Shreveport, Louisiana*

Static and statnamic load tests were performed on two 0.76-m-diameter drilled shafts installed through stiff to hard clays to tip in very dense sand (Wang et al. 1991). Test Shaft No. 2 was embedded to a depth of approximately 16 m, and Test Shaft No. 3 was embedded to a depth of about 11.3 m. In neither case did the statnamic load achieve plunging failure due to the lack of capacity of the device at the time (January 1991). Nevertheless, the data for Test Shaft No. 3 are included because of the availability of strain gage measurements along the shaft during both the static and statnamic tests. Soil conditions at test Shaft No. 3 consist of stiff to very stiff silty clays to a depth of about 8 m underlain by very dense fine silty sand. Undrained shear strength from unconfined compression tests in the clays averaged about 100 kPa, and standard penetration test resistance in the sand was around 100 b/ft (b/300 mm). Groundwater levels were above the top of the sand.

Presented in Figs. 29 and 30 are the load versus displacement plots for the static loading and subsequent statnamic loading of this shaft. A first look at the statnamic load versus displacement plot would immediately suggest that the full static soil resistance was not mobilized during this test because Area 4 is extremely small and the permanent displacement upon unloading is very

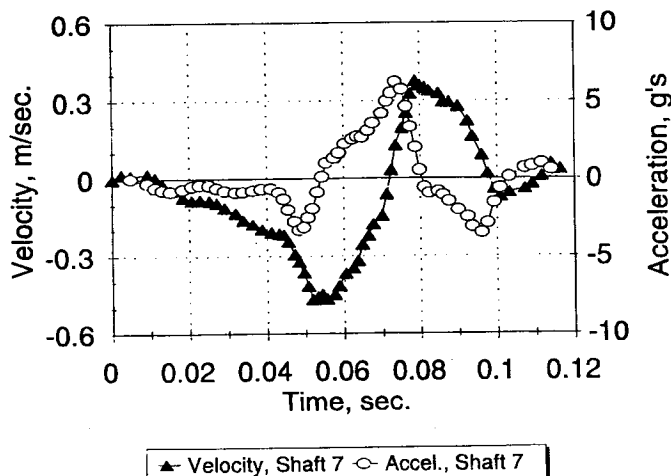


FIG. 28—Velocity and acceleration versus time, Shaft 7, College Station, TX.

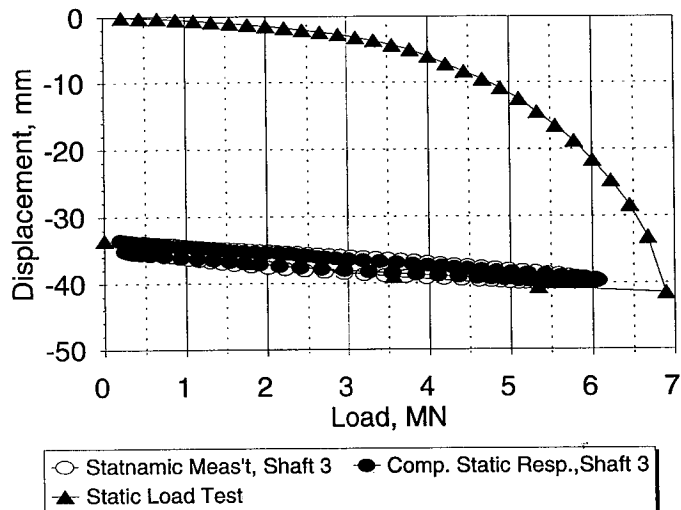


FIG. 29—Load versus displacement, Shreveport, LA.

small. However, the statnamic loading does appear to represent a reasonable reloading curve up to about 6 MN after the previous static loading to nearly 7 MN.

The measurement of particular interest at this site is the plot of load distribution along the shaft shown in Fig. 31 for a load on the shaft of about 5 MN. Note that the statnamic measurements (captured as a function of time during the loading) along the shaft have been adjusted for the expected phase lag related to the compression wave travel time along the shaft. These data suggest that the distribution of static soil resistance along the shaft during the statnamic loading is quite similar to that during a static load test.

*Summary of  $C_d$  Damping Factors*

Although the damping coefficient,  $C_d$ , is determined as a part of the data reduction process, it is of interest to summarize these computed coefficients for future reference. Presented in Table 1 are the damping coefficients that have been computed for these case studies using Eq 5. These data do not illustrate any particular pattern which can be attributed to soil type, but all are within reasonably close range. It should be noted that, within the general range of values shown, the computation of static soil resistance

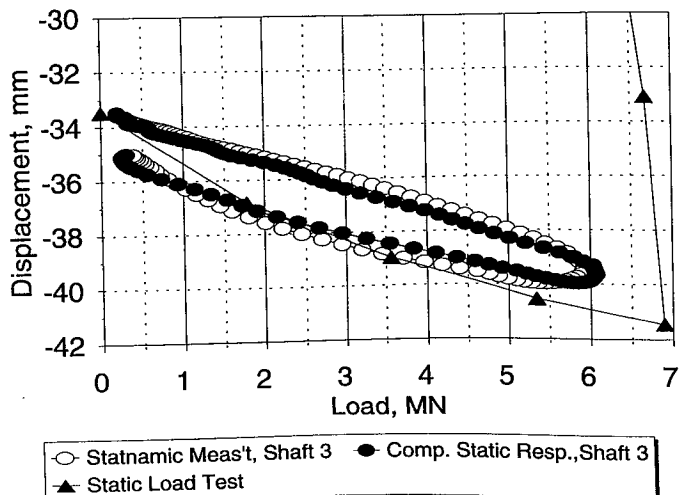


FIG. 30—Load versus displacement, Shreveport, LA.

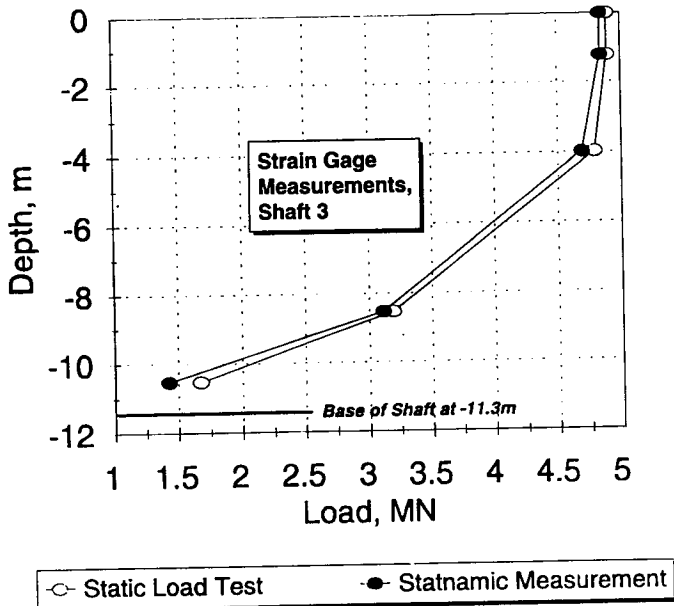


FIG. 31—Load distribution, Shreveport, LA.

from the statnamic data is not particularly sensitive to the  $C_d$  coefficient.

**Evaluation**

The results of the case studies of statnamic load tests provide a basis for defining the current state of the art with respect to this test procedure. Presented in Fig. 32 is a summary comparison of the computed static soil resistance from the statnamic measurements versus the maximum measured load from the static load tests on the same shaft. Although such a diagram does not indicate the suitability of the predicted load versus settlement plots shown on a case-by-case basis earlier, this plot graphically combines the case studies in this report.

The data in Fig. 32 illustrate the good agreement of the statnamic data with conventional static load tests for drilled shafts in sandy soil and the one test in soft clay (actually representing the “mud-

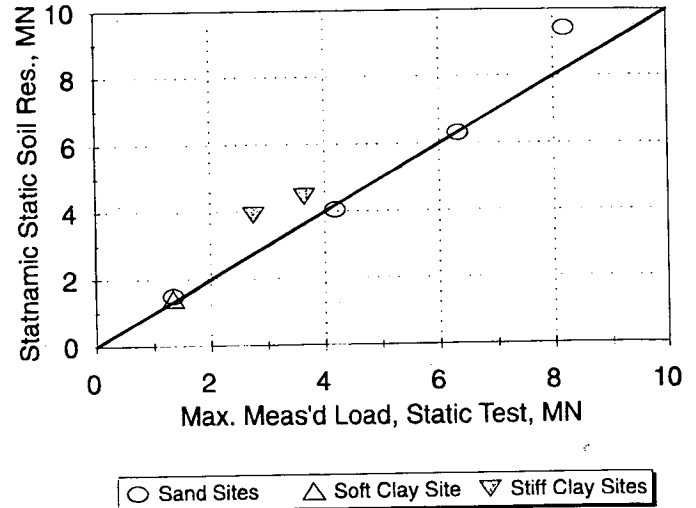


FIG. 32—Comparison of static load test versus statnamic comp. max. static soil resistance.

cake” defective shaft). The one data point that deviates from the otherwise near perfect agreement in sandy soils was on the New Mexico test shaft, which was subjected to load-unload-tensile load-reload, and it is quite possible that the comparison of statnamic and static was affected somewhat by the load history of this shaft.

For the two tests to failure in stiff clays, the statnamic data represent an overestimate of the conventional static load test capacity; the Shreveport data are not included since that test did not fully mobilize the static soil resistance. Although damping is accounted for in the analysis procedure of the statnamic measurements, it would appear that for these shafts in stiff, overconsolidated clay there is some additional effect related to the rapid loading in the statnamic. It could be that there is additional damping in these soils not adequately accounted for with the Middendorp procedure or that the static resistance mobilized during the relatively rapid rate of loading differs from the static resistance mobilized during a conventional test, which takes several hours. These stiff, overconsolidated clays would be expected to exhibit dilatancy during shear, and negative pore water pressures would be expected near the shaft/soil interface. This effect with the relatively plastic clays could account for more of a rate-dependent strength than for sandy soils with greater hydraulic conductivity. In softer clay soils, dilatancy and negative pore water pressures might not occur. It is clear that more research is needed into the loading rate effects in these clay soils as the above explanations can only be characterized as speculation without experimental measurements. Furthermore, two load tests in stiff clay soils are inadequate for broad generalizations.

The load settlement plots derived from the statnamic measurements appear to be quite good in almost all of the case histories analyzed using the Middendorp procedure. Most of the direct comparisons on drilled shafts reflect the differences between an initial loading and a reloading after some permanent set has occurred, and it is suggested that there need to be some load tests performed in which statnamic loading is followed by static loading rather than vice versa. However, the statnamic does appear to be a promising tool where load versus deflection response measurements are needed.

The load distribution along the shaft was similar for the statnamic and static loadings in the one case study where such data are available. Additional data of this type are needed for critical evalua-

TABLE 1— $C_d$  damping coefficients.

Site	Soil Type	$C_d$ , MN/m/s
I-40, Rio Puerco	Dry, clayey	-2.1
I-40, Rio Grande, test 1	Wet, silty sand	-2.6
I-40, Rio Grande, test 2	Wet, silty sand	-5.4
Auger Cast Piles, Barrie, Ontario	Wet, silty sand	-1.3
Cupertino, CA	Dry sand	-0.4
Texas A&M, shaft 4	Wet sand	-0.9
Texas A&M, shaft 2	Wet sand w/soft clay mudcake	.. .
Texas A&M, shaft 7	Stiff clay	-1.7
Shreveport, LA	Stiff clay over silty sand at base	-1.3

\*Note, insufficient acceleration and displacement data to accurately calculate; estimated at -0.4 for purposes of computing capacity.

tion of the device and test procedure with respect to the mobilized load transfer along the shaft. The limited data presented in this report suggest good agreement between statnamic and static loading. Note that additional data of this type are being generated in Europe (Middendorp 1992) and in Asia that may provide for a broader evaluation of the general test method.

### Conclusions

The use of the statnamic loading device combined with the Middendorp procedure for computation of the mobilized static soil resistance appears to be a viable alternative to conventional load testing, particularly for drilled shaft foundations. The loading is relatively quick and efficient, does not require a reaction frame, can be designed to generate the relatively large loads needed for testing drilled shafts, and does not pose a significant concern with respect to damaging the shaft from the impact of a blow. The comparisons with conventional static load tests outlined in this paper suggest that excellent agreement can be obtained in sandy soils, but the current evaluation procedure may tend to overpredict capacity by as much as 25 to 30% in stiff, overconsolidated clays. Load versus settlement response predicted from statnamic measurements was generally good, although most of the test data reflect a reloading curve rather than initial loading. The load distribution along the shaft was nearly identical to that of a conventional static loading in the one case for which such data were available.

### Acknowledgments

The author wishes to acknowledge the financial support of the Federal Highway Administration, Region 4, and the Auburn University Highway Research Center. Many people provided test data and offered helpful comments and suggestions, including Bob Horvath of McMaster University, Patrick Bermingham of Bermingham Corp., Mike Levine of New Mexico State Highway and Transportation Department, Jean-Louis Briaud of Texas A&M, Mike O'Neill of the University of Houston, Bengt Fellenius of the University of Ottawa, and Barry Berkovitz of FHWA; their cooperation and contributions are gratefully acknowledged.

### References

- Ballouz, M., Nasr, G., and Briaud, J. L., 1991, "Dynamic and Static Testing of Nine Drilled Shafts at Texas A&M University, Geotechnical Research Sites," report for Bell Bottom Foundation Co.
- Middendorp, P., 1992, "The First Statnamic Load Testing of Foundation Piles in Europe," *Seminar: Evolution in Experimentation for Constructions*, Centro Comune di ricerca di Ispra (VA), Italy.
- Middendorp, P., Bermingham, P., and Kuiper, B., 1992, "Statnamic Load Testing of Foundation Piles," *Proceedings, Fourth International Conference on Application of Stress-Wave Theory to Piles*, The Hague, pp. 581-588.
- Wang, S. T., Reese, L. C., O'Neill, M. W., and Majano, E., 1991, "Axial-Load Tests of Drilled Shafts on I-49/I-20 Interchange, Route I-49, Caddo Parish, Louisiana," report for Bell Bottom Foundation Co.

## Discussion on "Evaluation of Static Capacity of Deep Foundations from Statnamic Testing" by Dan Brown\*

**REFERENCE:** Goble, G. G., Rausche, F., and Likins, G., "Discussion on 'Evaluation of Static Capacity of Deep Foundations from Statnamic Testing' by Dan Brown," *Geotechnical Testing Journal*, GTJODJ, Vol. 18, No. 4, December 1995, pp. 493-498.

**KEYWORDS:** piles, drilled shafts, load tests, instrumentation, statnamic method

The author's careful review of the Statnamic method and the presentation of test data are of great value to the geotechnical profession. Since Statnamic is a patented method, it is difficult to obtain the independent evaluation that normally occurs when a new concept is presented. The discussers would like to comment on several points contained in the paper.

The developers of the Statnamic method have conceded (Middendorp et al. 1992) that Statnamic is really a dynamic event. The most recently proposed method of evaluation assumes that the test pile is rigid and examines the forces acting on the pile at the instant that motion stops. This approach was suggested by Eiber (1958) in laboratory research supervised by H. R. Nara at the Case Institute of Technology and was further developed in an extended project at Case sponsored by the Ohio Department of Transportation and the FHWA. The simplest version of the methods developed was published by Goble et al. (1967, 1970) and is identical with the method currently proposed for Statnamic. Later developments at Case abandoned the rigid body assumption for a more realistic and accurate elastic model.

The Statnamic test is fundamentally different from static tests in that *Statnamic uses a specified applied load* rather than the *imposed displacement that is applied by the static test*. In a static test, a volume of hydraulic fluid is pumped into the loading system, inducing an associated displacement. The load induced will depend on the stiffness of the pile and the test frame. When the load equals the strength of the pile soil system, pile displacements will continue to increase without any increase in load. In the Statnamic case, the total of the pile's static and dynamic soil resistance is much larger than the Statnamic mass, causing a much higher upward acceleration and displacement of the Statnamic mass while the pile has comparatively little downward movement. Thus, the explo-

sive gas pressure and the applied Statnamic force will only be slightly affected by the resistance characteristics.

The applied Statnamic force *must be in equilibrium* with the sum of the pile's static resistance *plus* the pile's velocity-related resistance *plus* the pile's acceleration-related inertia. Normally, both the static and dynamic resistances of the pile are not known in advance. Selecting a Statnamic force to achieve a significant permanent set after the test requires application of a Statnamic load larger than the sum of all resistance components. *Due to the relatively slow Statnamic load buildup, all static plus dynamic resistance forces occur more or less simultaneously, and the applied Statnamic force must be much larger than the pile's ultimate static load to achieve soil failure and could cause pile structural failure.* In normal impact dynamic testing, the load quickly reaches its full value; stress waves distribute the impact loading in time so that the applied force need only be similar to the pile's static capacity to achieve soil failure.

The damping coefficients,  $C_4$ , tabulated by the author, show a surprisingly large variability. In cases where Statnamic forces considerably larger than the static capacity are applied, high pile velocities are generated. In the data presented, the peak velocity ranged from 0.2 to 3.5 m/s, a range of more than an order of magnitude. If Shaft 2 at College Station is dropped, the largest maximum velocity is still 1.2 m/s. This large range of peak velocities may partially explain the large range of damping coefficients  $C_4$ . For sands, the range of damping coefficients is from -0.4 to -5.4. Clay sites have similar values and ranges. No clear relationship is observed. Coyle and Gibson (1970) in laboratory tests demonstrated that the peak dynamic resistance was a strongly nonlinear function of the velocity, a result confirmed by others (Heerema 1979; Litkouhi and Poskitt 1980). In fact, Janes (1995) presents results of Statnamic tests that show that the Statnamic damping "constant"  $C_4$  varied on the same pile by a factor of 3 when the applied Statnamic force was doubled.

During the loading phase, the loading rate can be controlled by the amount of explosive and reaction mass. However, the unloading rate is not controlled, and large decelerations are generated, occurring near the time of load evaluation by the Statnamic equilibrium point method. Thus, the inertia term correction in the Statnamic capacity analysis can be quite sensitive to high accelerations for large shafts with a large mass; the pile mass may be further increased by some undeterminable soil mass moving with the pile. In fact, the unloading phase is so short that the rigid body assumption is violated and stress waves are generated in the pile, causing large tension stresses. Several records presented by the

\*Published in the *Geotechnical Testing Journal*, Vol. 17, No. 4, December 1994, pp. 403-414.

<sup>1</sup>Professor emeritus, University of Colorado at Boulder, and principal, Goble Rausche Likins and Associates, Inc., Boulder, CO.

<sup>2</sup>President, Goble Rausche Likins and Associates, Inc., Cleveland, OH.

<sup>3</sup>President, Pile Dynamics, Inc., Cleveland, OH.

author clearly show this tension at the top of the shaft (due to upward inertia of the Statnamic device during rebound); tension in the shaft would be higher still due to the extra shaft mass. In general, damage cannot be detected in the Statnamic measurements due to the slow load application.

The results presented include several with obvious measurement problems. The data were obtained by measuring the displacement with a noncontact displacement measurement device that can be sensitive to vibrations from both ground and wind. Those measurements were then differentiated to obtain the velocity and a second time to get acceleration. The greatest accelerations occurred during the unloading phase, where the capacity is evaluated. Double differentiation to obtain acceleration magnitudes is an unreliable process, particularly when the displacement measurements are subjected to filtering in the signal conditioning and computation process, which introduces another variable, as the author points out. Most of the measurements indicate derived accelerations that are obviously incorrect in the early part of the record where some even have incorrect signs. Under these circumstances, the Statnamic inertia correction and capacity results become highly questionable.

The author notes that Cupertino Shaft 4 was not loaded to failure in either the static or the Statnamic case. For Texas A & M Shaft 2, the displacement measurement went out of range, so the point of zero velocity could not be determined as recommended. The selected  $C_4$  damping coefficient does not match either the other Texas A & M tests or other sites with similar soils. The test in Barrie, Ontario, also probably did not fail and the Statnamic test was not run on the static test pile, making the correlation results for this shaft questionable. These cases should be excluded from the correlation of Fig. 32.

It is unfortunate that the author did not have more data available since many more tests have been reported. The results presented by Janes et al. (1994) from tests conducted at the University of British Columbia Pile Research Site in the Fraser River Delta near

Vancouver, Canada are of interest. One of the results taken from that paper, Fig. 9, is shown here as Fig. 1. The pile was a steel pipe about 30 m long, driven closed ended through 15 m of soft organic silty clay and 15 m of dense, fine-to-medium sand into a normally consolidated clayey silt with sand layers. The load deflection curve followed the static test curve quite well up to the static failure load at about 1100 kN. The Statnamic "static" load then increases to over 2000 kN, about double the ultimate capacity measured by a static load test, and then unloads with near full rebound. *If the Statnamic test does not cause true soil failure and a reasonable permanent set, then the Statnamic test becomes unreliable and may grossly overpredict capacity.*

In Janes et al. (1994), it is concluded that the test *must* be carried to a soil failure condition typified by the author's Fig. 3. Results from Cupertino and Shreveport should not have been included since soil failure clearly was not achieved. In these cases, the Statnamic "capacity" was determined solely by the Statnamic force applied. To achieve soil failure, it may be necessary in some cases to load the pile substantially above the pile static capacity due to the dynamics. In three of the four remaining valid correlation cases presented (Rio Puerco, Albuquerque, and Texas A & M Shaft 7), Statnamic significantly overpredicted the capacity ultimate loads from the static tests.

The Statnamic name may be misleading to the engineer not familiar with the dynamics involved in this test method. *The test is clearly dynamic and must cause significant permanent pile set after the test to be useful in determining ultimate "static" loads.* Due to the test's potential for large overpredictions, it should always be correlated with static test results. To be of value, tests of this relatively high cost should produce results that are as reliable as the static test. This does not appear to be the case from the Statnamic results presented. There is very little "Class A" data available. Additional data, independent evaluation, and perhaps

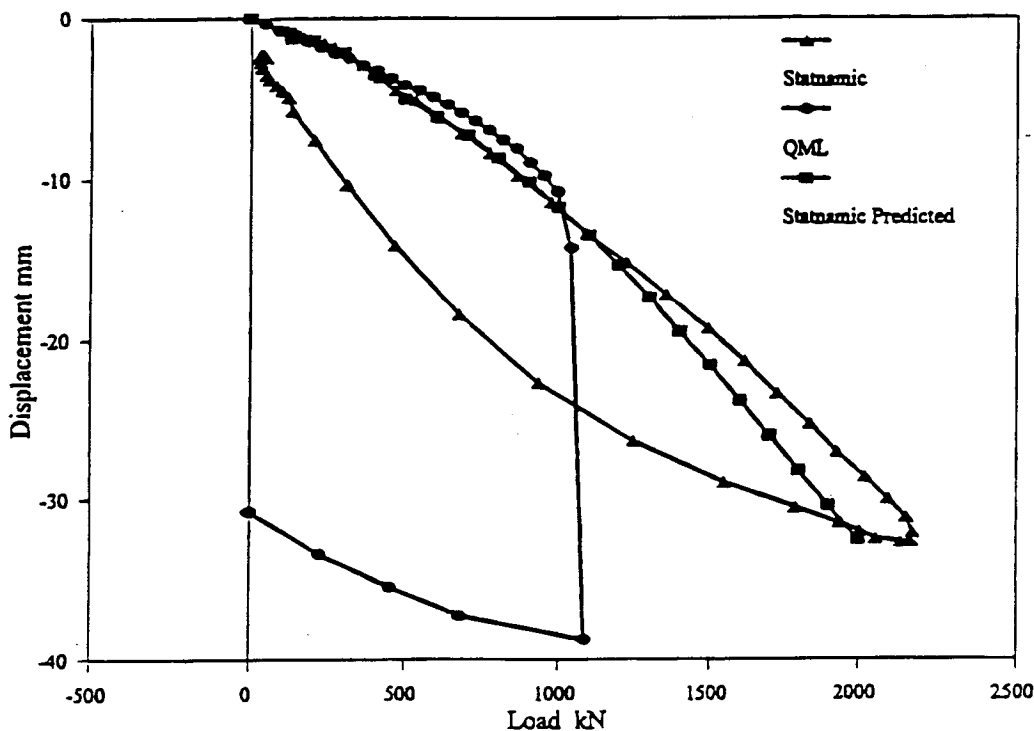


FIG. 1—Statnamic and static test results for Fraser River Pile 5 (Janes 1994).

method modification will be required before Statnamic can be used without a calibrating static test.

## References

- Coyle, H. M. and Gibson, G. C., 1970, "Empirical Damping Constants for Sands and Clays," *Journal of Soil Mechanics and Foundations Division, ASCE*.
- Eiber, R. J., 1958, "A Preliminary Laboratory Investigation of the Prediction of Static Pile Resistances in Sand," Master's thesis, Department of Civil Engineering, Case Institute of Technology, Cleveland, OH.
- Goble, G. G., Scanlan, R. H., and Tomko, J. J., 1967, "Dynamic Studies on the Bearing Capacity of Piles," Highway Research Record No. 167, Bridges and Structures, April.
- Goble, G. G. and Rausche, F., 1970, "Pile Load Test by Impact Driving," Highway Research Record No. 333.
- Heerema, E. P., 1979, "Relationship between Wall Friction, Displacement, Velocity, and Horizontal Stress in Clay and in Sand for Pile Driveability Analysis," *Ground Engineering*, January.
- Janes, M., Sy, A., and Campanella, R., 1994, "A Comparison of Statnamic and Static Load Tests on Steel Pipe Piles in the Fraser Delta," *Proceedings, Eighth Annual Symposium on Deep Foundations*, Vancouver Geotechnical Society, Vancouver, British Columbia.
- Janes, M., 1995, "Statnamic Load Testing of Bridge Pier Foundations in North America," *Proceedings, Thirty-first Symposium on Engineering Geology and Geotechnical Engineering*, Utah State University, Logan, Utah.
- Litkouhi, S. and Poskitt, T. J., 1980, "Damping Constants for Pile Driveability Calculations," *Geotechnique*, Vol. 30, No. 1.
- Middendorp, P., Bermingham, P., and Kuiper, B., 1992, "Statnamic Load Testing of Foundation Piles," *Proceedings, Fourth International Conference on the Application of Stress-Wave Theory to Piles*, The Hague, The Netherlands, Balkema, Rotterdam.

## Closure

*D. Brown*—The author acknowledges the comments of discussers Goble, Rausche, and Likins and is grateful for their interest and efforts in contributing to the exchange of ideas relating to this subject. The author's response to these comments and the results of some additional analyses follow.

The author acknowledges the earlier work relating to the use of the zero velocity point in evaluating dynamic response. The rigid body assumption is made as a part of the evaluation of Statnamic measurements according to the Middendorp procedure. As will be described subsequently in this closure, this assumption imposes severe limitations on the interpretation of the data in some instances and is an area in which future development is needed. The author is not aware of any claims that the Statnamic is a static procedure.

The author agrees that the Statnamic test provides for a specific applied load (approximately) rather than a specific applied displacement and that the test load must be greater than all static plus dynamic forces (more or less simultaneously) to achieve soil failure. Thus, the method requires a large applied force, but the system is designed to provide a relatively large force in an efficient manner without damaging the shaft or pile. In fact, there are many forces in nature that are applied with a loading frequency that is roughly similar to that of the Statnamic, such as ship impact and seismic loadings; an understanding of the deep foundation response during a Statnamic loading event offers promise in improving our understanding of foundation response during such extreme event loadings. The measured response of piles during high-strain dynamic impact testing also provides insight into deep foundation behavior that is not obtained in any other way, particularly with long slender driven piles. Impact testing produces high-frequency

excitation in which the effects of stress wave propagation dominate the shaft response. These techniques differ in fundamental ways, and foundation engineers would be well advised to make maximum use of all available tools to improve designs at a particular site.

The paper presented by the author utilized many of the North American test data that were available at the time of the study (summer, 1993) for which reliable data were available, static load tests on the same or similar shafts were available, and for which soil failure appeared to be achieved, or nearly so. The Shreveport test was included because of the availability of strain measurements below grade, even though soil failure was not achieved. This technique is relatively new and evolving, and more test data have become available subsequently, including those results reported by Janes and referenced by the discussers. As has been the case regarding high-strain dynamic testing, soil damping factors are observed to vary with soil and pile types and experience is required to be able to predict a range of expected values in advance of testing.

The discussers noted, as has the author, the need for improved reliability in measurements of acceleration during the Statnamic loading event. More recent Statnamic tests have included the addition of an accelerometer measurement that is sensitive to the relatively low  $g$  forces that occur during Statnamic testing. The author has observed no evidence of large tension stresses in any shaft tested with the Statnamic device.

Some additional analytical investigations have been performed in order to examine the effect of damping factors, shaft inertia, wave propagation effects, and soil quake (displacement required to mobilize full static resistance) on the expected response and interpretation of the response during a Statnamic-type loading event. The author has conducted these numerical experiments on both a rigid body (using a simple code developed by the author) and on a realistic shaft model using the finite element computer code PAR (Pile Analysis Routines) (PMB Engineering 1988, 1994) developed for use in the analysis of offshore structures. The results of this study on a rigid body motion suggest that none of these effects, including velocity-dependent damping or soil quake values, would adversely affect the correct interpretation of the static load resistance using the Middendorp procedure. However, with the introduction of realistic elastic behavior in the foundation element, the limitations of the Middendorp procedure in some cases are apparent.

Analyses have been performed on a pair of idealized foundations typical of drilled shaft construction in the United States, consisting of 1.2-m-diameter concrete shafts that are either 12.2 or 24.5 m in length and installed into a uniform deposit of medium-stiff clay with an undrained shear strength of 48 kPa. In such a case, load resistance at relatively small displacements is primarily related to side friction along the shaft, and the soil is of a type that would be expected to develop relatively high damping resistance during a Statnamic loading event. Presented in Fig. 2 is a plot of the static load-displacement response of the model for the two shaft lengths and for two different quake values for side resistance. The 5-mm value is likely to be more realistic (in the author's experience), and the 12-mm value is intended to represent a "large quake" condition. Toe quake values of 5 and 10% of the shaft diameter were used in the two cases, respectively, however, the toe resistance serves to produce only a very small strain hardening in the load-displacement response as is evident from Fig. 2.

The shaft was loaded using a time-dependent force applied to the top node of the shaft in a manner intended to replicate approximately the Statnamic loading. This force consists of first

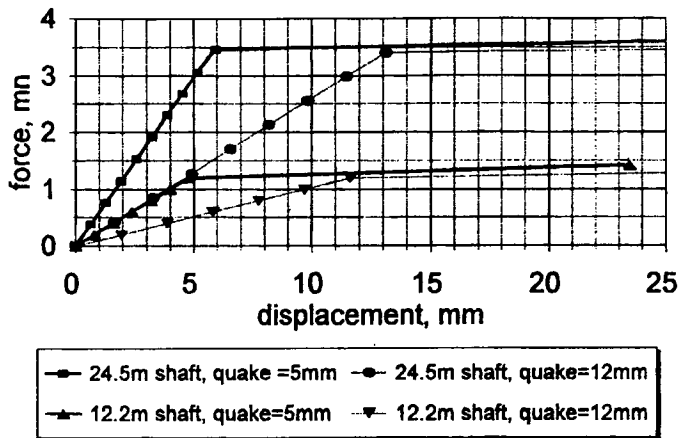


FIG. 2—Static load-displacement: 1.2-m-diameter shaft in med-stiff clay.

applying a small static force of between 5 and 10% of the peak force, followed by a ramp load that builds linearly to a maximum in a time of 0.050 s and drops linearly to zero in an additional 0.020 s. All analyses were carried out for a duration of 0.120 s to capture the post-loading event stresses in the shafts. The shaft models consist of linear elastic beam elements with a node spacing of approximately 1.5 m. The soil is modeled as a series of nonlinear springs and dashpots in a manner typical of wave equation analyses.

Presented in Fig. 3 is a plot of the force-displacement response of the model for the 12.2-m shaft with 5-mm side quake and the relatively substantial damping that would be expected for such soil. Also plotted is the static load-displacement response for the model and the interpreted static load-displacement response that would be obtained using the Middendorp procedure outlined in the paper. It is evident from this figure that the prediction of the maximum static resistance mobilized during the loading event is quite good, but the static load-displacement response leading up to that point is underpredicted. This underprediction at small displacements appears to be related to the adjustment that is made for inertia based upon the assumption of rigid body motion. Figure 4 presents a similar plot with the interpreted static resistance not including an adjustment for inertia [as is sometimes done with the Statnamic (Janes 1995) with the justification that the inertia term is small]. The exclusion of the inertia adjustment is seen to improve the load-displacement curve with a reduction in the maximum

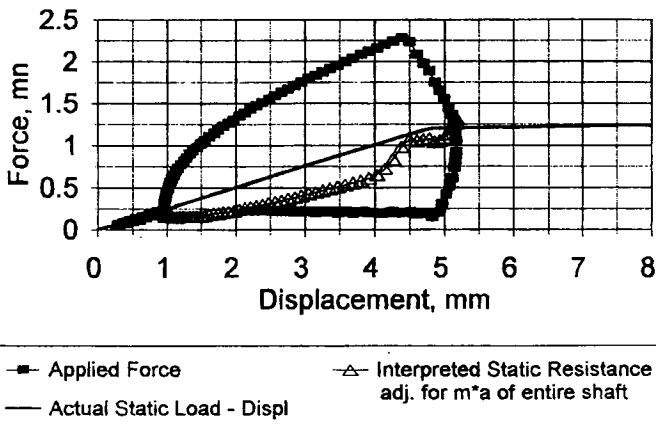


FIG. 3—PAR analysis of ramp load with damping: 12.2-m shaft, quake = 5 mm.

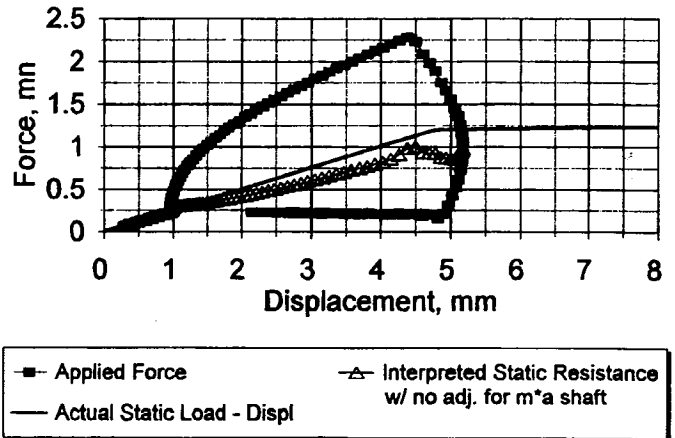


FIG. 4—PAR analysis of ramp load with damping: 12.2-m shaft, quake = 5 mm.

static resistance prediction. The inertia adjustment based upon rigid body motion clearly overstates the amount of force due to mass times acceleration effects in the early stages of the test because all of the mass is not yet moving with the velocity of the topmost node.

The data shown in Figs. 5 and 6 provide similar force-displacement plots of the same shaft with greater and lesser applied Stat-

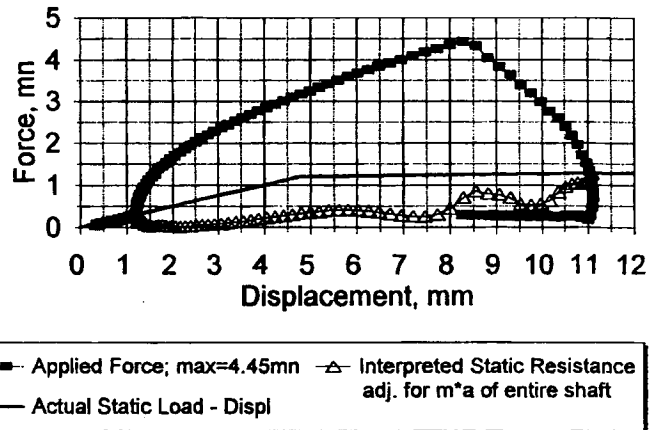


FIG. 5—PAR analysis of ramp load with damping: 12.2-m shaft, quake = 5 mm.

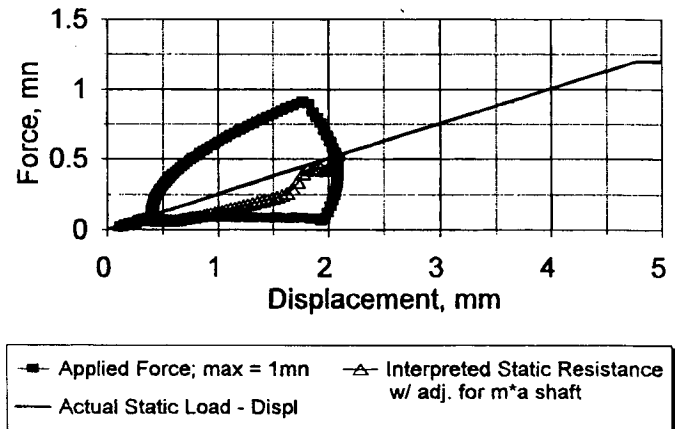


FIG. 6—PAR analysis of ramp load with damping: 12.2-m shaft, quake = 5 mm.

namic force in order to evaluate the effect of maximum peak force on the interpretation of the results using this procedure. In both cases, observations are similar to those described for the baseline case in which the maximum static resistance appears to be reliably predicted and the load-displacement curve up to the maximum load is underpredicted. In the case shown in Fig. 6 in which the shaft did not achieve full mobilization of the static resistance, the maximum static resistance was not overestimated by the Middendorp procedure.

Analyses of the longer shaft with otherwise similar quake and damping values is presented in Fig. 7. This shaft illustrates the influence of wave-propagation effects on the interpretation of the Statnamic loading using the Middendorp procedure. For this length of shaft, the compression wave travel time is on the order of 0.007 s, a significant value with respect to estimating zero velocity points based on a measured displacement at the top of the shaft. The maximum static resistance is clearly seen to be overestimated using this method. Ignoring the inertia adjustments would tend to improve the prediction, but such an approach is not justified. Provided in Figs. 8 and 9 are similar plots for this shaft with increased damping resistance and larger soil quake values, respectively. Larger damping appears to make the error in estimated static resistance worse. Larger soil quake values, even such that the full static resistance is not mobilized, does not appear to result in a worse error even though the static resistance is still somewhat overestimated.

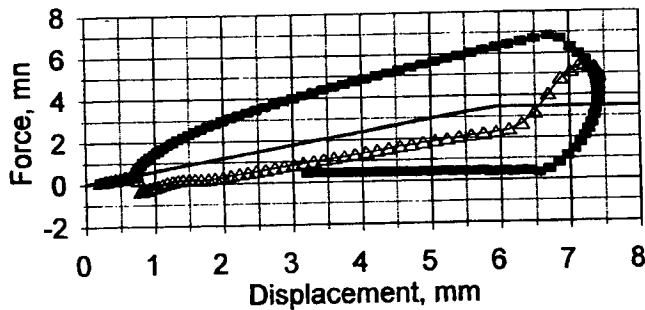


FIG. 7—PAR analysis of ramp load with damping: 24.5-m shaft, quake = 5 mm.

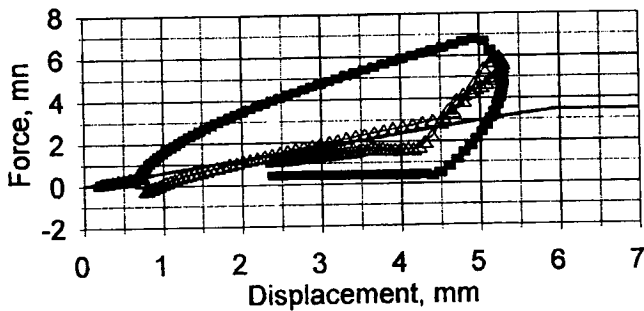


FIG. 8—PAR analysis of ramp load with damping: 24.5-m shaft, quake = 5 mm, damping X2.

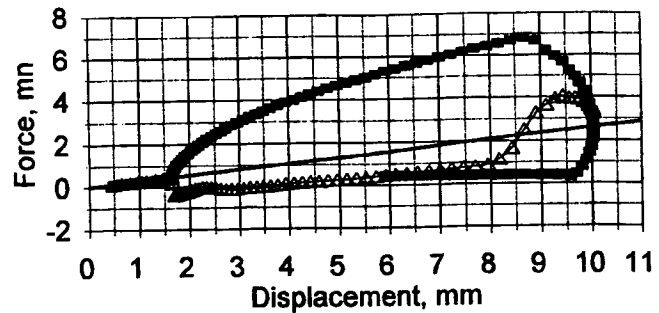


FIG. 9—PAR analysis of ramp load with damping: 24.5-m shaft, quake = 12 mm.

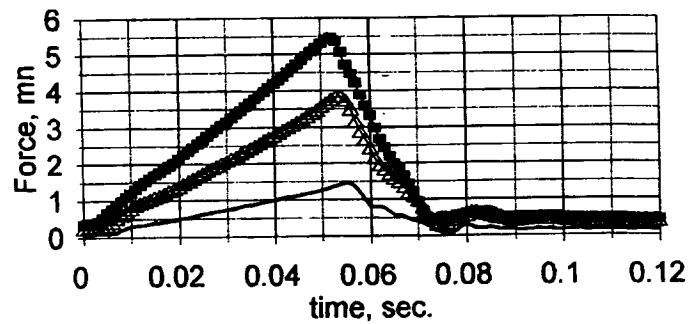


FIG. 10—PAR analysis of ramp load with damping: 24.5-m shaft, quake = 5 mm.

The author's conclusion from these simple analytical studies is that there is a need for an improved interpretation procedure for use with the Statnamic method. The errors and overpredictions of capacity in some instances noted by the discussers appear to be due primarily to the fact that the rigid-body assumption in the Middendorp procedure described in the paper is not appropriate for long slender shafts, especially in soils that may have high damping resistance. The data provided by Janes and referenced by the discussers was a long slender pipe pile in alluvial silts that represents just such a case. The fact that the Middendorp procedure has been shown to work well in some cases is likely due to the use of the procedure in cases where relatively short shafts have been analyzed or where soil damping is relatively low. In such cases, the limitations of the method are likely to be quite small.

These studies suggest that the load level or soil quake is not likely to be a factor that would contribute to poor predictions of static resistance. As with any measurement, if the load is insufficient to mobilize the full static resistance, one can only estimate the static resistance that was mobilized with that loading.

With respect to the discussor's implication that Statnamic loading may cause damage to the shaft, the finite element studies described in this closure support the author's contention that a Statnamic loading should not result in significant tensile stresses in the shaft. Presented in Fig. 10 are data from one typical case illustrating the force-time history at several locations within the

test shaft. These data are similar to field strain measurements that have been observed by the author subsequent to preparation of the paper. Compressive stresses in the shaft during a Statnamic loading may be somewhat higher than in a conventional static loading due to the need to overcome inertia and damping, but are likely to be less severe than with high-strain impact testing. This fact is one of the advantages of a Statnamic loading when applied to cast-in-situ piles or drilled shafts that are not designed to withstand high driving stresses as would a driven pile.

The Statnamic loading procedure has some inherent advantages over conventional static or high-strain dynamic testing. Large loads can be achieved, the full shaft or pile is displaced downward simultaneously, and the stresses imposed are relatively modest. The damping resistances that are mobilized during the test may be of great interest for some extreme event loadings. The Statnamic testing procedure is relatively new and has not enjoyed the long incubation period of more established dynamic testing methods.

The author agrees with the discussers that improved interpretation procedures are needed with evaluation of additional test data. However, the author is optimistic that continued development can provide engineers with another tool that can improve foundation design effectiveness and reliability.

#### *Acknowledgments*

The author wishes to acknowledge the generosity of PMB Engineering, San Francisco, California and Gordon A. Bang for the use of their finite element software in performing the analyses described in this closure.

#### **References**

- PMB Engineering, Inc., 1988, "User's Manual, PAR, Pile Analysis Routines."
- PMB Engineering, Inc., 1994, "User's Update Manual, PAR, Pile Analysis Routines."